# AN ANALYTICAL AND EXPERIMENTAL STUDY OF PERFORMANCE ON JATROPHA BIODIESEL ENGINE

by

*Thirunavukkarasu GANAPATHY, Rakesh Parkash GAKKHAR, and Krishnan MURUGESAN*

Original scientific paper
UDC: 662.756.3:519.876.2/.5
DOI: 10.2298/TSCI0903069G

*Biodiesel plays a major role as one of the alternative fuel options in direct injection diesel engines for more than a decade. Though many feed stocks are employed for making biodiesel worldwide, biodiesel derived from domestically available non-edible feed stocks such as Jatropha curcas L. is the most promising alternative engine fuel option especially in developing countries. Since experimental analysis of the engine is pricey as well as more time consuming and laborious, a theoretical thermodynamic model is necessary to analyze the performance characteristics of jatropha biodiesel fueled diesel engine. There were many experimental studies of jatropha biodiesel fueled diesel engine reported in the literature, yet theoretical study of this biodiesel run diesel engine is scarce. This work presents a theoretical thermodynamic study of single cylinder four stroke direct injection diesel engine fueled with biodiesel derived from jatropha oil. The two zone thermodynamic model developed in the present study computes the in-cylinder pressure and temperature histories in addition to various performance parameters. The results of the model are validated with experimental values for a reasonable agreement. The variation of cylinder pressure with crank angle for various models are also compared and presented. The effects of injection timing, relative air fuel ratio and compression ratio on the engine performance characteristics for diesel and jatropha biodiesel fuels are then investigated and presented in the paper.*

Key words: *biodiesel, Jatropha curcas L., thermodynamic model, performance, diesel engine*

## Introduction

Biodiesel has been identified versatile fuel and promising potential diesel alternative for diesel engine applications because of its characteristics such as renewable, biodegradable, comparable energy density, easily producible, domestically available, non toxic, low emissions, energy independent, and self reliant. Hence it has been in use for the past more than a decade, although vegetable oil was employed by Rudolf Diesel in 1900 for his first ever diesel engine fuel [1]. The lower cost of the petroleum diesel has so far attracted the world to use it as fuel in diesel engines until now. But nowadays due to global political turmoil and other reasons the cost of petroleum diesel has been increasing and crossing over the cost of some varieties of vegetable oil. The developing countries can not afford to edible oil feed stocks for biodiesel production as they are not self-sufficient for their culinary needs. Therefore these countries make their biodiesel from non-edible feed stocks. Jatropha biodiesel is one of the most promising options among these. Although there are many experimental studies of jatropha biodiesel engines, there is an obvious lack of thermodynamic models for analyzing their performance characteristics analytically.

In general the thermodynamic models depend on the equations which are based on energy conservation laws from the first law of thermodynamics. These models are classified into three categories *viz*, zero-dimensional, phenomenological, and quasi-dimensional models. In zero-dimensional models, geometric features of the fluid motion can not be predicted as flow modeling is absent in it. In phenomenological models, some details in addition to energy conservation equations can be built-in for each phenomenon. Whereas in quasi-dimensional models specific geometric features can also be incorporated to the basic thermodynamic equations [2, 3].

In the present work, a thermodynamic model has been developed to study the performance characteristics of the Jatropha biodiesel engine. Using this model, pressure, temperature, and other required properties are computed numerically for every crank angle step chosen. The engine friction and heat transfer computations are also incorporated in the model using empirical equations obtained from experiments reported in the literature. The ignition delay is also taken into account in the combustion model. The heat release calculations of the model are based on Wiebe's empirical functions taking the premixed and diffusive combustions into account.

This two zone thermodynamic model is applied for the design and operating data of a vertical single cylinder, four stroke, air cooled, direct injection diesel engine. Initially the engine is operated with diesel fuel, subsequently jatropha biodiesel is used as fuel and then the results are compared and analyzed. The model has then been validated by an experimental analysis carried out at the author's laboratory. The results of the present model are also compared with those of zero-dimensional single zone thermodynamic model reported in the literature [4].

Gardner *et al.* [5] developed a mathematical model and analyzed the effect of compression ratio on the different performance parameters such as thermal efficiency, mechanical efficiency, ignition delay, mean effective pressure, maximum cylinder pressure, mechanical friction, and blow by. Harris *et al.* [6] accurately predicted the fuel consumption, torque and power of the different diesel engines using their universal mathematical model. Low heat rejection diesel engine was analyzed comprehensively using two zone combustion models and different heat transfer models by Tamilporai *et al.* [7] to simulate the engine heat release, cylinder peak pressure and temperature, and heat transfer details on zonal and cumulative basis. Shroff *et al*. [8] developed mathematical models of diesel engine to simulate and optimize the thermodynamic processes. Annand [9] proposed an empirical formula to calculate the heat transfer in the cylinders of reciprocating internal combustion engines. Way [10] presented methods to calculate the gas composition and thermodynamic properties in engines. The mathematical models are also developed for use in spark ignition engines to analyze various combustion parameters and performances [11, 12]. Literatures report that artificial neural networks based models have also been developed by many researchers [13-17] for studying the performances and emissions of compression ignition and spark ignition engines, and different characteristics of fuel used thereof.

## Thermodynamic model description

A two zone thermodynamic model has been developed to study the performance of vertical, single cylinder, four stroke, air cooled direct injection, compression ignition engine fueled with diesel and jatropha biodiesel. The model is based on the first law of thermodynamics equation. The staring point for the thermodynamic calculations is selected at the instant at which the intake valve shuts up and the compression process commences. Since at this instant both intake as well as exhaust valves are closed, the thermodynamic system is a closed one. Hence energy equation for the closed cycle period can be applicable, which has been obtained from energy conservation law. This equation states that the rate of change of internal energy is as a result of rate of change of heat release, heat transfer, and work transfer. This closed cycle simulation program models the compression, combustion, and expansion processes in the engine. During these processes the properties in the cylinder are calculated for each crank angle step chosen.

The compression process is analyzed by using ideal gas equation and polytropic process law. During combustion process, the rate of heat release is calculated using an empirical equation of double Wiebe's function. This heat release function adequately administers the combustion of two zones namely premixed and diffusive zones. The ignition delay is also taken into account in the model and it is calculated by using the Wolfer's relation. The compositions of the gases are determined during the expansion process. The heat transfer is accounted for throughout the closed portion of the cycle. These calculations are based on Pflaum's relation. The exhaust and intake processes are also analyzed by the cycle simulation with the gas exchange processes. The model can predict the power output of the engine more close to the actual experimental values only if it takes into account the various frictional losses. Hence the various empirical equations proposed by Bishop [18] have been incorporated in the model to account for various frictional power losses.

### *First law of thermodynamics equation*

The energy equation according to first law of thermodynamics for the present model can be written in differential form as:

$$\frac{\mathrm{d}u}{\mathrm{d}\varphi} \quad \frac{\mathrm{d}Q}{\mathrm{d}\varphi} \quad \frac{\mathrm{d}W}{\mathrm{d}\varphi} \tag{1}$$

where the first term in eq. (1) represents the rate of change of internal energy of the system, the second term is meant for the rate of change of heat, and the last term is the rate of change of mechanical work done by the system on the boundary. Equation (1) after modification and substitution for various terms is written as:

$$m\frac{\mathrm{d}u}{\mathrm{d}\varphi} \quad \frac{\mathrm{d}Q_{\mathrm{hr}}}{\mathrm{d}\varphi} \quad \frac{\mathrm{d}Q_{\mathrm{ht}}}{\mathrm{d}\varphi} \quad \frac{\mathrm{d}W}{\mathrm{d}\varphi} \tag{2}$$

$$m\frac{\mathrm{d}u}{\mathrm{d}\varphi} \quad \frac{\mathrm{d}Q_{\mathrm{hr}}}{\mathrm{d}\varphi} \quad hA\frac{\mathrm{d}T}{\mathrm{d}\varphi} \quad \mathrm{R_u}\, T\frac{\mathrm{d}V}{\mathrm{d}\varphi} \tag{3}$$

where $m$ is the mass [kg], $\mathrm{d}u/\mathrm{d}\varphi$ – the rate of specific internal energy [$\mathrm{kJkg^{-1}deg^{-1}}$], $\mathrm{d}Q_{\mathrm{hr}}/\mathrm{d}\varphi$ – the rate of combustion heat release [$\mathrm{kJdeg^{-1}}$], $\mathrm{d}Q_{\mathrm{ht}}/\mathrm{d}\varphi$ – the rate of heat transfer from gases to walls [$\mathrm{kJdeg^{-1}}$], $\mathrm{d}W/\mathrm{d}\varphi$ – the rate of work done [$\mathrm{kJdeg^{-1}}$], $h$ – the convective heat transfer coefficient [$\mathrm{Wm^{-2}K^{-1}}$], $A$ – the surface area of the heat transfer [$\mathrm{m^2}$], $\mathrm{R_u}$ – the universal gas constant 8.314 kJ/kmolK, $T$ – the instantaneous temperature [K] at any crank angle ($\varphi$), $\mathrm{d}V/\mathrm{d}\varphi$ – the incremental change in cylinder volume [$\mathrm{m^3deg^{-1}}$], and $\varphi$ – the angular displacement with respect to bottom dead centre [deg].

### *Cylinder geometry*

The basic geometry of the diesel engine cylinder is shown in fig. 1. It is illustrated in terms of cylinder bore diameter ($D$), length of stroke ($L$), length of connecting rod ($l$), and compression ratio ($r_c$). The displacement volume $V_d$ is swept out as the piston moves from the bottom dead centre (BDC) to the top dead centre (TDC). The instantaneous engine cylinder volume at any crank angle position ($\varphi$) is given by:

$$V(\varphi) \quad V_d \quad \frac{r_c}{r_c \quad 1} \quad \frac{1 \quad \cos\varphi}{2} \quad \frac{l}{2a} \quad \frac{1}{2}\sqrt{\left(\frac{2l}{L}\right)^2 \quad \sin^2\varphi} \tag{4}$$

where $\varphi = 0$ ° when the piston is at BDC during the start of compression stroke and

$$\frac{dV}{d\varphi} \quad \frac{V_d}{2} \quad \frac{1}{2} \frac{\sin 2\varphi}{\sqrt{\left(\frac{2l}{L}\right)^2 \quad \sin^2\varphi}} \quad \sin\varphi \tag{5}$$

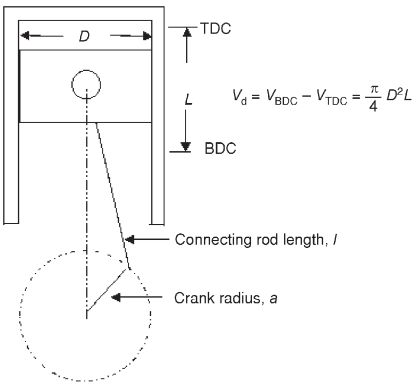


**Figure 1. Engine cylinder geometry**

*Compression and expansion processes*

The variation of pressure and volume for every degree crank angle is calculated during the compression process. The heat transfer from the cylinder gases to the walls is calculated from the start of compression to the start of combustion using an empirical formula [3]. Defining BDC during the compression process as zero degrees, the compression process begins at 30° after it. The initial conditions in the cylinder at this time are close to the conditions in the intake. The intake conditions are given as input data along with atmospheric conditions. The mass of the gas in the cylinder is calculated using the ideal gas equation. This defines the state at the start of the compression process. The cylinder gas composition at this state consists of air and residual gases. The model then steps through the cycle in every crank angle degree increments. A polytrophic process calculates the cylinder conditions throughout the compression and expansion processes with indexes of $k_r$ and $k_p$, respectively. For the compression stroke the composition in the cylinder is $N_a$ [kmol] of air and $N_x$ [kmol] of residual gases. During the expansion stroke the composition $N_p$ [kmol] of products of combustion is given by:

$$N_p = N_a + N_x + N_f \tag{6}$$

where $N_f$ is the kilo moles of fuel injected during the injection process. The mole fractions of the product gases are calculated based on the relative air fuel ratio.

*Exhaust and intake processes*

For exhaust and intake processes also called gas exchange processes, a control volume analysis with mass and energy conservations gives the model equations as given below. The exhaust gas is assumed to behave like ideal gas in the present model.

$$\frac{\mathrm{d}p}{\mathrm{d}\varphi} = \left[\gamma_{\mathrm{p}} p \left(\frac{1}{m}\frac{\mathrm{d}m}{\mathrm{d}\varphi} - \frac{1}{V}\frac{\mathrm{d}V}{\mathrm{d}\varphi}\right)\right]_{\mathrm{exhaust}} \tag{7}$$

$$\frac{\mathrm{d}p}{\mathrm{d}\varphi} = \left[\gamma_{\mathrm{r}} p \left(\frac{\mathrm{R}T_{\mathrm{a}}}{V}\frac{\mathrm{d}m}{\mathrm{d}\varphi} - \frac{P}{V}\frac{\mathrm{d}V}{\mathrm{d}\varphi}\right)\right]_{\mathrm{intake}} \tag{8}$$

$$\frac{\mathrm{d}m}{\mathrm{d}\varphi} = A p_0 \sqrt{\frac{2\gamma}{\mathrm{R}T(\gamma-1)}\left(\frac{p}{p_0}\right)^{\frac{\gamma-1}{\gamma}}\left[\left(\frac{p}{p_0}\right)^{\frac{\gamma-1}{\gamma}}-1\right]} \quad \text{when} \quad \frac{p}{p_0} > \left(\frac{\gamma+1}{2}\right)^{\frac{\gamma-1}{\gamma}} \tag{9}$$

$$\frac{\mathrm{d}m}{\mathrm{d}\varphi} = A p \sqrt{\frac{\gamma}{RT}\left(\frac{2}{\gamma+1}\right)^{\frac{\gamma+1}{\gamma-1}}} \quad \text{when} \quad \frac{p}{p_0} \le \left(\frac{\gamma+1}{2}\right)^{\frac{\gamma}{\gamma-1}} \tag{10}$$

where, for exhaust process, $p$ is the cylinder pressure [bar], and $p_0$ – the exhaust manifold pressure [bar], and for intake process, $p$ is the intake manifold pressure [bar] and $p_0$ – the cylinder pressure [bar], $\gamma$ is the specific heat capacity ratio of the gas, $A$ – the effective area of opening for the gas flow [m$^2$], $\gamma_{\mathrm{p}}$ – the specific heat ratio of products, $\gamma_{\mathrm{r}}$ – the specific heat ratio of reactants, $m$ – the mass of the gas [kg], and $\mathrm{d}p/\mathrm{d}\varphi$ – the pressure drop due to heat transfer [bar deg$^{-1}$].

### *Combustion model*

The combustion process can be described with varying complexity and accuracy. Normally the degree of complexity is decided based on the number of zones in which the cylinder has been divided. In the present modeling, the combustion process is taken to occur in two zones, namely premixed zone and diffusive zone. The two stage behavior of combustion heat release rate curves are commonly identified as premixed combustion and diffusive combustion regardless of the operating conditions. Adequate curve fitting to this two stage combustion rate curves resulted in double Wiebe's function which is given by eq. (11). The heat release rate in these zones is calculated by using this equation. The different empirical heat release rate constants proposed by Wiebe's [19] are used for each zone of the combustion process:

$$\begin{aligned}\frac{\mathrm{d}Q_{\mathrm{hr}}}{\mathrm{d}\varphi} = {} & 6.9\frac{Q_{\mathrm{p}}}{\varphi_{\mathrm{p}}}(M_{\mathrm{p}}+1)\left(\frac{\varphi}{\varphi_{\mathrm{p}}}\right)^{M_{\mathrm{p}}}\exp\left[-6.9\left(\frac{\varphi}{\varphi_{\mathrm{p}}}\right)^{M_{\mathrm{p}}+1}\right] + \\ & 6.9\frac{Q_{\mathrm{d}}}{\varphi_{\mathrm{d}}}(M_{\mathrm{d}}+1)\left(\frac{\varphi}{\varphi_{\mathrm{p}}}\right)^{M_{\mathrm{d}}}\exp\left[-6.9\left(\frac{\varphi}{\varphi_{\mathrm{d}}}\right)^{M_{\mathrm{d}}+1}\right]\end{aligned} \tag{11}$$

### *Ignition delay*

The time delay between the start of injection and the start of combustion (the start of detectable heat release) is defined as the ignition delay period. In the combustion model the ignition delay is also taken into account. The ignition delay period is calculated by integrating Wolfer's relation [3] using trapezoidal rule.

$$t \quad \frac{A}{p^n}\exp\ \frac{E_\mathrm{A}}{\mathrm{R_u}\,T}\ , \quad {}_{t_{inj}}^{t_{ign}}\ \frac{1}{t}\ \mathrm{d}t \quad 1 \tag{12}$$

$$_{t_{inj}}^{t_{ign}}\ \frac{\mathrm{d}t}{t(p,T)} \quad \frac{1}{A_{t_\mathrm{inj}}}\ {}_{t_{inj}}^{t_{ign}}\ \frac{\mathrm{d}t}{\dfrac{1}{p(t)^n}\exp\ \dfrac{E_\mathrm{A}}{\mathrm{R_u}\,T(t)}} \tag{13}$$

*Heat transfer*

Heat transfer has become inevitable in any internal combustion engine so as to maintain cylinder walls, cylinder heads and pistons at secure in service temperatures. Heat is transferred from or to the working fluid during every part of each cycle. The rate of heat transfer is given by the eq. (14).

$$\frac{\mathrm{d}Q_\mathrm{ht}}{\mathrm{d}\varphi} \quad hA\frac{\mathrm{d}T}{\mathrm{d}\varphi} \quad hA(T_\mathrm{g} \quad T_\mathrm{w})\Delta t \tag{14}$$

where $h$ is the convective heat transfer coefficient [$\mathrm{Wm^{-2}K^{-1}}$], $A$ – the internal surface area of cylinder volume [$\mathrm{m^2}$], $T_\mathrm{w}$ – the inside surface wall temperature [K], and $T_\mathrm{g}$ – the working fluid temperature [K]. The empirical formula proposed by Pflaum [3] for the heat transfer in the interior surface of cylinder volume given by eq. (15) has been used in the model to compute the heat transfer coefficient:

$$h = \sqrt{p_\mathrm{g}}\,T_\mathrm{g}\mathrm{f}(C_\mathrm{m}) \qquad \text{where} \qquad \mathrm{f}(C_\mathrm{m}) = 3 \quad 2.57\{1 - \ \exp[\ (1.5 - 0.415\ C_\mathrm{m})]\} \tag{15}$$

$p_\mathrm{g}$ is the pressure [bar], $C_\mathrm{m}$ – the mean piston speed [m min.$^{-1}$], and $T_\mathrm{g}$ – the mean gas temperature [K].

*Frictional losses*

Some portion of the power developed in the engine cylinder has been absorbed to overcome friction in various parts. In addition, to surmount inlet and throttling losses and pumping losses, a part of the power output is consumed. The empirical relations proposed by Bishop [18] are employed in the present model to calculate the various frictional losses. The various losses that are taken into account are mean effective pressure lost to overcome friction due to the gas pressure behind rings, friction due to wall tension of rings, friction due to piston and rings, inlet and throttling losses, friction due to valve gear, bearing friction, pumping losses, combustion chamber and wall pumping losses, and blow-by loss.

*Gaseous mixture properties*

Generally in combustion process, fuel and oxidizer react to produce products of different composition. A general formula for the composition of fuel can be represented as $C_nH_mO_r$. The five species of combustion products considered in the present model include $CO$, $CO_2$, $H_2O$, $N_2$, and $O_2$. The chemically correct amount of oxygen required for combustion per mole of fuel can be given by the equation:

$$n_{\mathrm{O_2}} \quad n \quad \frac{m}{4} \quad \frac{r}{2} \tag{16}$$

where, $n$, $m$, and $r$ are the number of moles of carbon, hydrogen, and oxygen atoms in one mole of fuel, respectively.

The various properties of the gaseous mixture such as, specific heat capacity at constant pressure, internal energy, and enthalpy are functions of gas temperature and its composition. The gaseous mixture composition depends on the relative proportions of fuel and air fed to the engine, fuel composition, and completeness of combustion. If the combustion system is adiabatic and the process of combustion is complete then the temperature of gaseous mixture, being the maximum value, is called adiabatic flame temperature. The adiabatic flame temperature of the gaseous mixture is computed using the iterations of Newton-Raphson method because it converges more rapidly than the other methods. The following equations are used to calculate the various properties of the mixture [2].

$$U_1 = k_1 + (k_2 - \mathrm{R})T + k_3\ln(T), \quad U_2 = k_4 + (k_5 - \mathrm{R})T + k_6\ln(T) \tag{17}$$

$$H_1 = k_1 + k_2T + k_3\ln(T), \quad H_2 = k_4 + k_5T + k_6\ln(T) \tag{18}$$

$$C_{\mathrm{p1}} = k_2 + \frac{k_3}{T}, \quad C_{\mathrm{p2}} = k_5 + \frac{k_6}{T} \tag{19}$$

$$C_{\mathrm{v1}} = (k_2 - \mathrm{R}) + \frac{k_3}{T}, \quad C_{\mathrm{v2}} = (k_5 - \mathrm{R}) + \frac{k_6}{T} \tag{20}$$

where $k_1$, $k_2$, and $k_3$ are coefficients of polynomial equation for $400 \le T \le 1600$, $k_4$, $k_5$, and $k_6$ are coefficients of polynomial equation for $1600 \le T \le 6000$, $U$ is the internal energy [kJkmol$^{-1}$], $H$ – the enthalpy [kJkmol$^{-1}$], $C_\mathrm{p}$ – the specific heat capacity at constant pressure [kJkmol$^{-1}$K$^{-1}$], $C_\mathrm{v}$ – the specific heat capacity at constant volume [kJkmol$^{-1}$K$^{-1}$], R – the universal gas constant [kJkmol$^{-1}$K$^{-1}$], suffixes 1 and 2 of $U$, $H$, $C_\mathrm{p}$, and $C_\mathrm{v}$ are for lower and higher temperature ranges, respectively, and $T$ – the adiabatic flame temperature [K].

## Computational procedure

A computer code has been developed using Fortran Power Station version 4.0 and the various equations of the thermodynamic model described in the section *Thermodynamic model description* are solved numerically. Then the Fortran program code is executed on a Pentium-IV personal computer. The fuel parameters *viz*, mole numbers of carbon, hydrogen, and oxygen, heating value, molecular weight of the fuel and cut off ratio, the engine geometrical parameters (bore, stroke length, connecting rod length, piston skirt length, and number of piston rings), molecular weight of gaseous products and the various constants used in the model are defined in the Data Subroutine. Compression ratio, relative air fuel ratio, Wiebe's constants for premixed and diffusive combustion zones, engine speed, inlet conditions, and atmospheric conditions are given as input parameters through an input file. The number of moles of exhaust gas constituents are calculated from the air fuel ratio and molecular formula of the fuel employed. The various properties of the gaseous constituents are calculated as a function of temperature for each degree crank angle. Newton-Raphson method is used to solve for adiabatic flame temperature of the gaseous mixture. The cylinder volume at every degree crank angle is computed from the cylinder geometry. The ignition delay is calculated with help of Wolfer's model. The heat release due to combustion in the two zones is computed using the double Wiebe's heat release correlation. Pflaum's heat transfer coefficient model has been employed to determine the heat transfer between the gases and the engine cylinder walls. Then the temperature of the gas in the cylinder at each crank angle step is computed using Runge-Kutta fourth order algorithm. Finally the pressure of the gas in the cylinder at every crank angle step is calculated. Then the frictional power losses are calculated using Bishop's empirical relations. The various outputs of the computer program are pressure, temperature, volume at each crank angle step, maximum pressure of the cycle, maximum temperature of the cycle, indicated mean effective pressure, brake mean effective pressure, indicated power, brake power, indicated thermal efficiency, brake thermal efficiency, volumetric efficiency, and mechanical efficiency.

## Experimentation

In the present investigation a vertical, single cylinder, four stroke, direct injection, air cooled, Greaves Cotton – 4360, diesel engine has been used. The specifications of the engine are listed in tab. 1. The schematic diagram of the experimental set up employed in the present work is shown in fig. 2. The engine was loaded by an AVL alpha-20 eddy current dynamometer rated at 20 kW. An AVL-GM12D miniature pressure transducer connected with the charge amplifier and an eight channel OROS OR38 data acquisition system were used to measure the cylinder pressure histories. An AVL Angle Encoder-333 was used to detect TDC. AVL fuel consumption meter was used to measure the fuel consumption rate. The diesel and Jatropha biodiesel, whose properties are listed in tab. 2, were used in the experimental tests. All the experimental tests were carried out at a speed of 1500 rpm, 60% load and injection timing of 27° before TDC.

**Table 1. Engine specifications**

| | |
|---|---|
| Make | Greaves cotton |
| Model | 4360 |
| Bore | 82 mm |
| Stroke | 68 mm |
| Displacement | 359 $cm^3$ |
| Specific fuel consumption | 0.299 kg/kWh |
| Rated power | 5 kW |
| Rated speed | 3600 rpm |

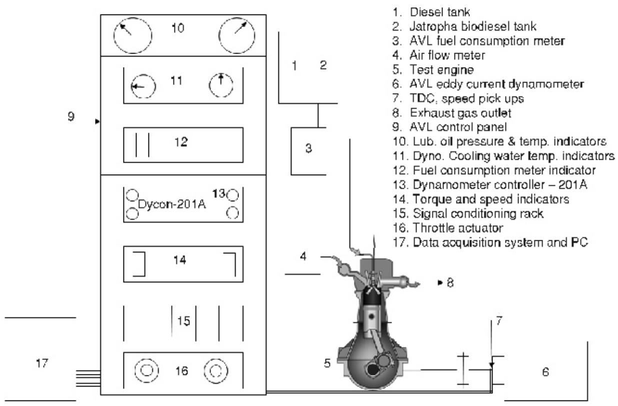


**Figure 2. Schematic diagram of the experimental setup**

**Table 2. Properties of diesel and jatropha biodiesel**

| Property | Diesel | Jatropha biodiesel |
|---|---|---|
| Molecular formula | $C_{10}H_{22}$ | $C_{20}H_{24}O_3$ |
| Specific gravity | 0.845 | 0.880 |
| Calorific value [$kJkg^{-1}$] | 42480 | 38450 |
| Kinematic viscosity (cSt.) at 40 °C | 3.9 | 4.8 |
| Flash point [°C] | 50 | 175 |

## Results and discussions

The present model is tested with petroleum diesel and Jatropha biodiesel as fuels in the diesel engine. However, the code has been developed in such a way that it is suitable for any hydrocarbon fuel of molecular formula $C_nH_mO_r$. The performance parametric studies can be carried out and the effects of variation of different parameters on the performance of the diesel engine can be analyzed and investigated by using the model.

In the present investigation, the effects of variation of compression ratio, relative air-fuel ratio, and injection timing on the performance characteristics of the diesel engine fueled with diesel and jatropha biodiesel, are analyzed using the present two zone model and their results are reported. The instantaneous in-cylinder pressure with respect to crank angle is also computed using the model and compared with experimental values and single zone model. Figures 3 and 4 show that the instantaneous in-cylinder pressure values predicted by the present model are closer to the experimental values than that of the single zone model for diesel as well as Jatropha biodiesel fuels. Though all the pressure variation curves seem to be in similar trends, it can be observed that the trend of the single zone model, for the crank angle duration of about 170° CA to 190° CA, is quite different (fig. 3 and 4) and hence its peak pressure value and its angle of occurrence are apparently shifted away from the experimental one. This is because of the limitation that the single zone model can not handle premixed and diffusive combustions. However with the present model the predicted cylinder pressure values are comparatively closer to the experimental, because premixed and diffusive combustions are adequately handled and in addition, the heat transfer calculations are better in this model.

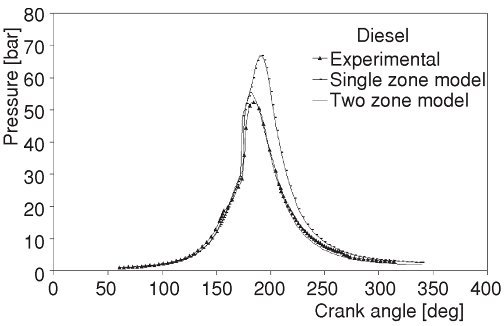


**Figure 3. Comparison of cylinder pressures of diesel**

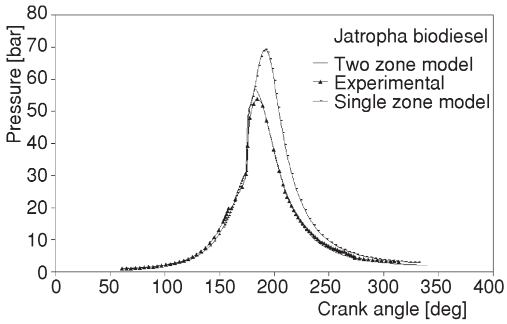


**Figure 4. Comparison of cylinder pressures of jatropha biodiesel**

### *Injection timing*

Figures 5 to 9 show the effects of injection timing on brake thermal efficiency, mechanical efficiency, volumetric efficiency, brake mean effective pressure, and peak temperature and their comparison between jatropha biodiesel and diesel fueled engine. It can be noted that the highest brake thermal efficiency is obtained at the rated injection timing (27° before TDC) and increase or decrease of this timing, slightly lowers the brake thermal efficiency for diesel as well as for Jatropha biodiesel (fig. 5). It is shown in fig. 6 that the same trend is followed in mechanical efficiency also. However, the

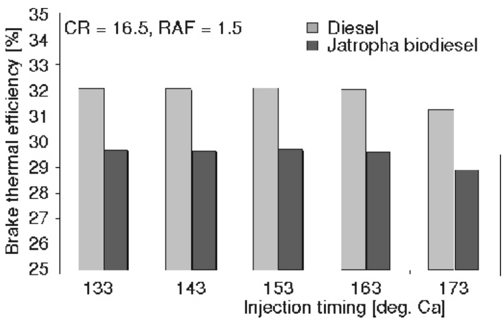


**Figure 5. Effect of injection timing on brake thermal efficiency**

brake thermal efficiency of diesel at any injection timing is greater than that of Jatropha biodiesel, whereas the mechanical efficiency is in the other way round. The respective reasons are, Jatropha biodiesel has lower calorific value due to its oxygen content and better lubricating characteristic compared to that of diesel. Hence the model predicts that diesel engine can effectively be operated with Jatropha biodiesel at an injection timing of 27° before TDC.

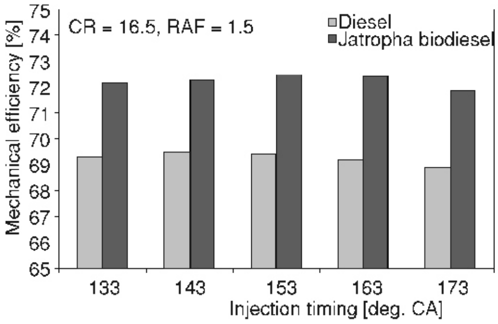


**Figure 6. Effect of injection timing on mechanical efficiency**

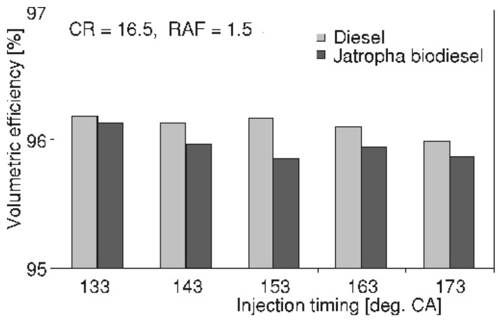


**Figure 7. Effect of injection timing on volumetric efficiency**

Volumetric efficiency is a measure of the effectiveness of induction process (gas exchange process) of four stroke cycle diesel engine. In general it is affected by fuel type, engine design, and engine operating parameters. Figure 7 shows the effect of injection timing on volumetric efficiency of the engine tested in the model. It may be observed that the injection timing has little effects on volumetric efficiency and it is almost consistent for both fuels. The same trends are seen for brake mean effective pressure also (fig. 8). However, the retardation of injection timing resulted in lower peak temperature of the cycle with both the fuels is shown in fig. 9. But the peak temperature of the Jatropha biodiesel is greater than that of diesel and this may be because, the Jatropha biodiesel having higher bulk modulus, leading to earlier injector needle lift and results in earlier fuel delivery to the chamber, compared to that of diesel.

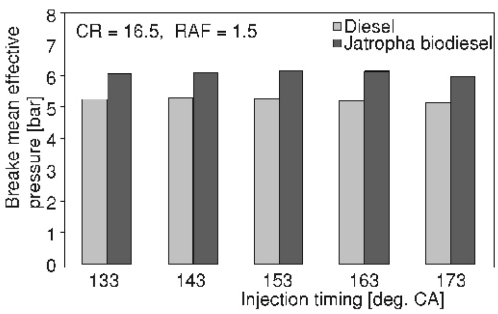


**Figure 8. Effect of injection timing on brake mean effective pressure**

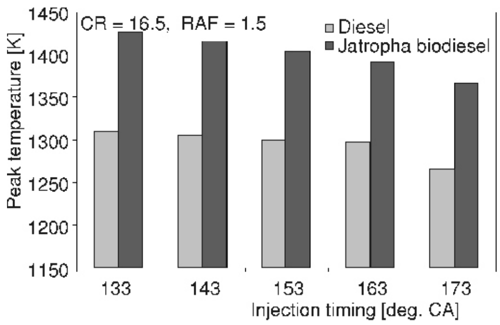


**Figure 9. Effect of injection timing on peak temperature**

*Compression ratio (CR)*

As the compression ratio is increased, the gaseous mixtures are compressed to high pressure in the compression process, which is shown in fig. 10. The variation of the pressure inside the combustion chamber for different compression ratios of jatropha biodiesel fueled engine is presented in fig. 10 and the same trends are obtained in the case of diesel fueled engine also. It is indicated in fig. 11 that the increase in compression ratio results in increased thermal efficiency with both the fuels. It can also be noted that this increasing rate of brake thermal efficiency in the case of jatropha biodiesel as well as of diesel is almost the same. However the brake thermal efficiency of jatropha biodiesel is always less than that of diesel fuel at any value

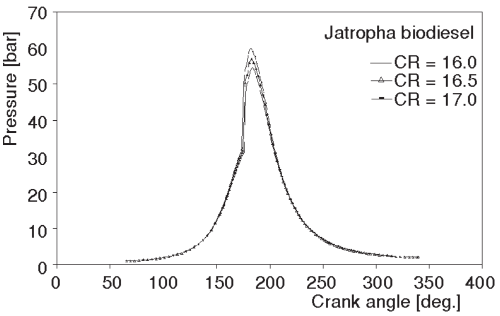


**Figure 10. Effect of compression ratio on cylinder pressure**

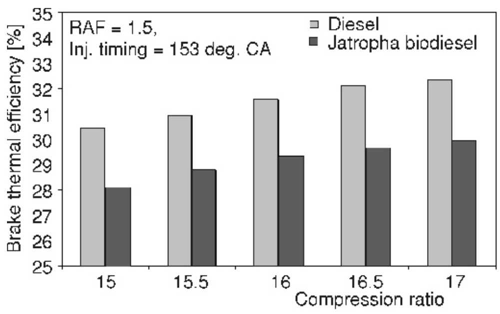


**Figure 11. Effect of compression ratio on brake thermal efficiency**

of compression ratio. This may be because of its inefficient combustion process. Figure 12 shows that mechanical efficiency increases with the increase of compression ratio for both the fuels. Although the rate of increase of mechanical efficiency is not substantial, it is found to be significant between compression ratios of 16.0 and 16.5. However, with jatropha biodiesel, the mechanical efficiency is significantly higher than that of diesel and this indicates that frictional power losses with jatropha biodiesel is less due to its better lubricity value.

The effect of compression ratio on brake mean effective pressure is shown in fig.13. It can be seen that as the compression ratio increases, the brake mean effective pressure of both the fuels increases. Also at any compression ratio the brake mean effective pressure of jatropha biodiesel is always greater than the diesel fuel operation, which proves again that there are lower frictional power losses with jatropha biodiesel operation. As the compression ratio is increased, the gaseous mixtures are compressed to high pressure in the compression process, which also leads to higher temperatures. The high pressure and temperature of the mixtures increases its burning rate, leading to

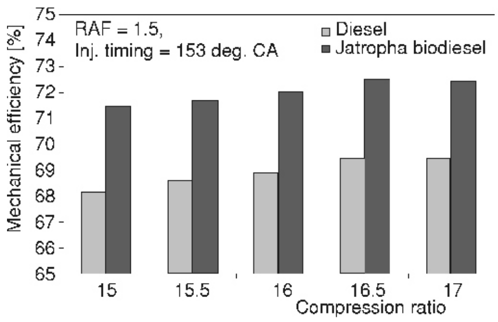


**Figure 12. Effect of compression ratio on mechanical efficiency**

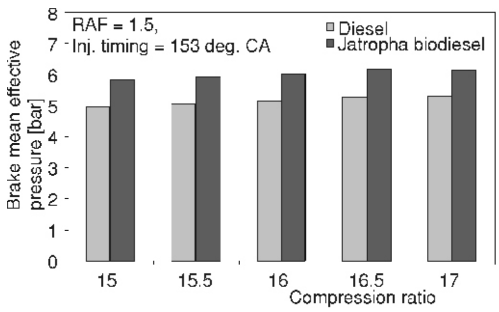


**Figure 13. Effect of compression ratio on brake mean effective pressure**

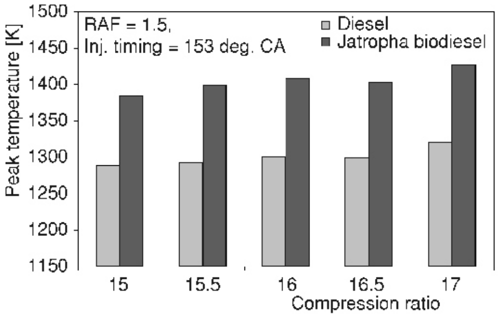


**Figure 14. Effect of compression ratio on peak temperature**

higher peak temperature which is shown in fig. 14. Also it can be seen that the peak temperature of the jatropha biodiesel is greater than that of diesel. This may be due to its advanced injection of jatropha biodiesel because of its higher bulk modulus compared to that of diesel.

### *Relative air-fuel ratio (RAF)*

The effectiveness of air utilization in combustion is well represented by relative air-fuel ratio. Its effects on the brake mean effective pressure and peak temperature are analyzed with the present model. The effect of relative air-fuel ratio on brake mean effective pressure is shown in fig. 15. It is shown that as the relative air-fuel ratio increases, the brake mean effective pressure decreases for diesel as well as for Jatropha biodiesel. This is because the mixture becomes leaner for the increased relative air-fuel ratio, leading to lower thermal energy release and hence results in lower brake mean effective pressure. However, the brake mean effective pressure is greater, as expected, in the case of jatropha biodiesel for any value of relative air-fuel ratio. Figure 16 shows that the peak temperature is reduced for an increased relative air-fuel ratio for both fuels. But the peak temperature of Jatropha biodiesel is greater than that of diesel for any value of relative air-fuel ratio. This may be due to the reason that Jatropha biodiesel, having oxygen content in the molecule, approaches complete combustion and in turn more energy release that results in higher peak temperature than that of the diesel fueled engine.

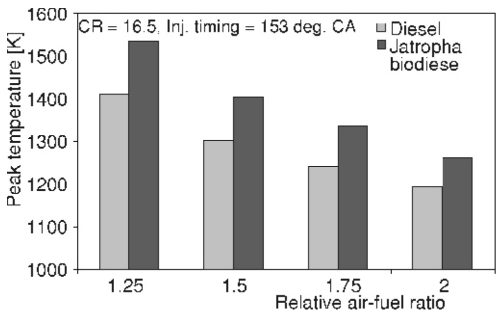


**Figure 15. Effect of relative air-fuel ratio on brake mean effective pressure**

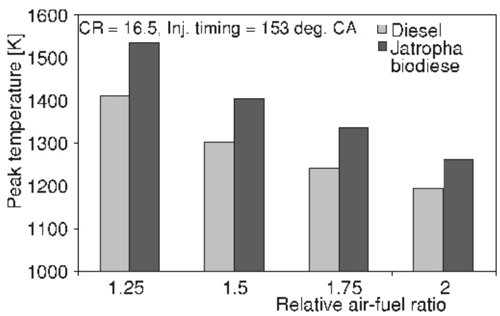


**Figure 16. Effect of relative air-fuel ratio on peak temperature**

### *Comparison of calculated and experimental cylinder pressure*

Figure 17 shows the calculated and experimental cylinder pressure variations with respect to crank angle. The numerically computed values of instantaneous pressure and experimentally measured values are compared for jatropha biodiesel as well as for diesel fuel operation at the same operating conditions. The trends of the cylinder pressure characteristic curves for Jatropha biodiesel and diesel models and experimental are almost similar in nature. Also the predictions of the model are very close to the experimental one. However, the peak pressure val-

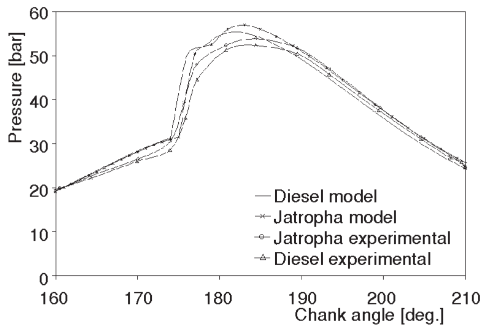


**Figure 17. Comparison of calculated and experimental cylinder pressure**

ues, respectively, for diesel and Jatropha biodiesel models, 55.402 bar, 56.95 bar occur at 2° and 3° crank angle after TDC.

## Conclusions

A two zone thermodynamic model is developed and the effects of operating parameters on the performance of the engine are studied. The results showed that for both the fuels, any change in the rated injection timing decreased the brake thermal and mechanical efficiencies, while retarded timing decreased the peak temperature. The increase in compression ratio increased all the above parameters, while increase in relative air-fuel ratio decreased brake mean effective pressure and peak temperature with both the fuels. The in-cylinder pressure histories computed by the model for the diesel and Jatropha biodiesel fueled diesel engine are closer to the experimental pressure data than that of the single zone model results. Hence, it is concluded that the two zone thermodynamic model can be used to predict the performance characteristics of the Jatropha biodiesel fueled diesel engine.

## Acknowledgments

The first author is thankful to the Ministry of Human Resources and Development, Government of India, for providing the fellowship for pursuing this research work at Indian Institute of Technology Roorkee, India.

## References

[1] Knothe, G., Dunn, R. O., Bagby, M. O., Biodiesel: The Use of Vegetable Oils and their Derivatives as Alternative Diesel Fuels, Oil Chemical Research, National Centre for Agricultural Utilization Research, Agricultural Research service, U. S Department of Agriculture, Peoria, Ill., USA
[2] Heywood, J. B., Internal Combustion Engine Fundamentals, McGraw-Hill, New York, USA, 1988
[3] Ganesan, V., Computer Simulation of Compression Ignition Engines, University Press (India) Ltd., Hyderabad, India, 2000
[4] Ramadhas, A. S., Jayaraj, S., Muraleedharan, C., Theoretical Modeling and Experimental Studies on Biodiesel-Fueled Engine, *Renewable Energy, 31* (2006), 11, pp. 1813-1826
[5] Gardner, T. P., Henein, N. A., Diesel Starting: A Mathematical Model, SAE 880426, 1988
[6] Harris, H. D., Pearce, F., A Universal Mathematical Model of Diesel Engine Performance, *J. Agric. Engng Res*., *47* (1990), 1, pp. 165-176
[7] Tamilporai, P., *et al*., Simulation and Analysis of Combustion and Heat Trabsfer in Low Heat Rejection Diesel Engine Using Two Zone Combustion Model and Different Heat Transfer Models, SAE 2003-01-1067, 2003
[8] Shroff, H. D., Hodgetts, D., Simulation and Optimization of Thermodynamic Processes of Diesel Engine, SAE 740194, 1974
[9] Annand, W. J. D., Heat Transfer in the Cylinders of Reciprocating Internal Combustion Engines. *Proceedings Instn Mech Engrs., 177*, (1963), 36, pp. 973-996
[10] Way, R. J. B., Methods for Determination of Composition and Thermodynamic Properties of Combustion Products for Internal Combustion Engine Calculations, *Proceedings Instn Mech Engrs.,190* (1977), 60/76, pp. 687-697

[11] Catania, A. E., *et al*., A Refined Two-Zone Heat Release Model for Combustion Analysis in SI Engines, *Proceedings*, 5th International Symposium on Diagnostics and Modeling of Combustion in Internal Combustion Engines (COMODIA 2001), Nagoya, Japan, 2001, pp. 2-18
[12] Wu, Y.-Y., Chen, B.-C., Hsieh, F.-C., Heat Transfer Model for Small-Scale Air-Cooled Spark-Ignition Four-Stroke Engines, *International Journal of Heat and Mass Transfer, 49* (2006), 21-22, pp. 3895-3905
[13] Canakci, M., Erdil, A., Arcaklioglu, E., Performance and Exhaust Emissions of a Biodiesel Engine, *Applied Energy, 83* (2005), 6, pp. 594-605
[14] Arcaklioglu, E., Celikten, I., A Diesel Engine's Performance and Exhaust Emissions, *Applied Energy, 80* (2005), 1, pp. 11-22
[15] Sayin, C., *et al*., Performance and Exhaust Emissions of a Gasoline Engine Using Artificial Neural Network, *Applied Thermal Engineering, 27* (2007), 1, pp. 46-54
[16] Korres, D. M., *et al*., A Neural Network Approach to the Prediction of Diesel Fuel Lubricity, *Fuel, 81* (2002), 10, pp. 1243-1250
[17] Yuanwang,D., *et al*., An Analysis for Effect of Cetane Number On Exhaust Emissions from Engine with Neural Network, *Fuel, 81* (2002), 15, pp. 1963-1970
[18] Bishop, I. N., Effects of Design Variables on Friction and Economy, *SAE Transaction, 73* (1965), pp. 334-358
[19] Miyamoto, N., Chikahisa,T., Murayama, T., Description and Analysis of Diesel Engine Rate of Combustion and Performance Using Wiebe's Functions, SAE 850107, 1985

Authors' affiliations

*T. Ganapathy* (**corresponding author**)
Internal Combustion Engines Laboratory,
Mechanical and Industrial Engineering Department,
Indian Institute of Technology Roorkee,
Roorkee 247667, India
E-mail: tganappathi@yahoo.co.in

*R. P. Gakkhar, K. Murugesan*
Internal Combustion Engines Laboratory,
Mechanical and Industrial Engineering Department,
Indian Institute of Technology Roorkee, India

Paper submitted: July 15, 2008
Paper revised: May 21, 2009
Paper accepted: July 10, 2009